Macromolecular Materials and Engineering
Open Access
www.mame-journal.de

# Thiol-ene Reaction as Reversible Covalent Bond for the Design of Shape-Memory Polymers

*Farhad Shohraty, Julian Hniopek, Josefine Meurer, Stefan Zechel, Michael Schmitt, Jürgen Popp, and Martin D. Hager**

**Besides a stable phase, shape-memory polymers require an additional switchable moiety. In addition to thermal transitions and supramolecular interactions, these units can also be based on covalent bonds. Herein, the use of the reversible thiol-ene reaction as reversible cross-linker for the design of shape-memory polymers is demonstrated. A facile route to polymer networks with a thiol-ene acceptor and a comonomer (butyl methacrylate or 2-ethylhexyl methacrylate) cross-linked by dithiols is introduced. The thermal and mechanical properties of the resulting polymers are characterized in detail. Hereby, the polymers feature excellent shape-memory behavior with fixity and recovery rates above 90%. This study shows that the thiol-ene cross-linker can function as both, the stable and the switchable structural moiety rendering the usage of a covalent cross-linker unnecessary. This partial reversibility can also be proven by temperature-depending Raman spectroscopy.**

## 1. Introduction

The implementation of nature-like functions into artificial materials is one major goal of current research.[1] The ability to change or to switch properties triggered by an external stimulus should be mentioned in this context.[2] This special ability can be used for the design of different functional materials, including self-healing polymers[3] and shape-memory polymers (SMPs), respectively.[4,5] Latter materials can change their shape upon being triggered by a specific stimulus, e.g., most commonly by elevated temperatures.[6] Hereby, the polymer can change its shape from a temporary shape to a permanent one. Thus, it is able to "memorize" the permanent shape, which is recovered due to the shape-memory effect.[7]

As a general design principle, SMPs feature two different building units. Firstly, the stable phase is responsible for the original form. Secondly, a switchable phase that is leading to the shape-memory effect.[8] The stable segment is providing stable cross-links within the polymer network and can be generated for instance by interpenetrating polymer networks,[9] chemical cross-links,[10] or stable crystalline domains.[11] In contrast, the reversible phase is featuring thermal transitions such as glass transition[12] or transitions between crystallization and melting[13] and can also be based on reversible covalent bonds[14,15] or dynamic supramolecular interactions.[16–18] All of these approaches have in common that the reversible units can be activated by a suitable trigger, such as temperature.

Compared to the other present approaches for the design of the switching moiety, dynamic covalent bonds have been used less frequently. However, these bonds feature the benefit of a relatively high chemical stability until the trigger is applied,[19] which is beneficial, e.g., in the context of prevention of creep.[20] Moreover, the switching can be decoupled from the thermal and mechanical properties of the polymer compared to classical $T_g$-switchable SMPs.

Several structural motifs have already been described in literature for the design of so-called covalent adaptable networks (CANs).[20] CANs can be divided into two principle mechanisms.[21] Whereas the associative mechanism relies on chemical bonds featuring the possibility of exchange reactions, dissociative CANs require the opening and closing of the reversible bond. Typical examples of associative reversible polymers are vitrimers,[22] as described by the groups of Leibler[23] and DuPrez[24] for example. The most common example for dissociative mechanism is the Diels–Alder cycloaddition, e.g., the reversible Diels–Alder reaction of furan and maleimide.[25]

Due to their reversibility, CANs are in between thermosets and thermoplastics considering their rheology.[26] In this context,

F. Shohraty, J. Meurer, S. Zechel, M. D. Hager
Laboratory of Organic and Macromolecular Chemistry (IOMC)
Friedrich Schiller University Jena
Humboldstr. 10, 07743 Jena, Germany
E-mail: martin.hager@uni-jena.de
F. Shohraty, J. Meurer, S. Zechel, M. D. Hager
Jena Center for Soft Matter (JCSM)
Friedrich Schiller University Jena
Philosophenweg 7, 07743 Jena, Germany
J. Hniopek, M. Schmitt, J. Popp
Institute of Physical Chemistry (IPC)
Friedrich Schiller University Jena
Helmholtzweg 4, 07743 Jena, Germany
J. Hniopek, M. Schmitt, J. Popp
Department Spectroscopy and Imaging
Leibniz Institute of Photonic Technology (IPHT) e. V.
Albert-Einstein-Straße 9, 07745 Jena, Germany

The ORCID identification number(s) for the author(s) of this article can be found under https://doi.org/10.1002/mame.202300002



**DOI: 10.1002/mame.202300002**

different types of bonds could already be used for the design of, e.g., self-healing and shape-memory polymers.[27–29]

Mainly, the Diels–Alder cycloaddition was integrated into polymers,[30] which already feature shape-recovery behavior such as polycaprolactone (PCL)[31] or polyurethanes.[32] Thus, the Diels–Alder unit acts as the stable phase. However, at higher temperatures the reversibility of the DA allows a reprocessing of the shape-memory polymer, which is hard to achieve for the classical nonreversible covalent cross-linking. Furthermore, the Diels–Alder unit was also used as reversible phase enabling triple shape-memory behavior. However, in these cases, a permanent cross-linker was used to stabilize the network.[33]

Thiol-ene chemistry represents an interesting alternative for the design of reversibly cross-linked SMPs. The reversibility has already been successfully demonstrated in self-healing polymers.[34,35] Interestingly, the reversible thiol-ene chemistry features an equilibrium between the open and the closed form, which is influenced by the temperature.[34] Due to this equilibrium, this cross-linker could potentially provide both, the stable as well as the reversible phase.

Herein, for the first time, we present the design of SMPs based on the reversible thiol-ene chemistry as switching moiety. Linear polymers or polymer networks containing a Michael acceptor, namely benzylcyanoacetamide, were reversibly cross-linked by dithiols. The thermal and mechanical properties were investigated by differential scanning calorimetry (DSC), thermogravimetric analysis (TGA), and thermo mechanical analysis (TMA). The resulting polymer networks showed excellent shape-memory ability.

Due to the special nature of the reversible thiol-ene reaction, no additional stable phase is required. This partial reversibility has also been demonstrated by Raman spectroscopic measurements.

## 2. Experimental Section

The materials and instrumentations as well as the synthesis of monomer **2** are summarized in the Supporting Information.

### 2.1. Synthesis of Polymers

#### *2.1.1. Linear Polymers*

Butyl methacrylate (BMA) for synthesis of **P1** to **P3**, or 2-ethylhexyl methacrylate (2-EHMA) for **P4** to **P6**, the desired amount of monomer **2** and 2,2'-azobis(2-methylpropionitrile) (AIBN) as initiator were dissolved in 10 mL dry *N,N*-dimethylformamide (DMF) in a 20 mL microwave vial. The exact amounts of all used monomers and reagents are summarized in Table S1 (see Supporting Information). The monomer-to-initiator ratio for all polymerizations was 100 to 1. The reaction mixture was purged with a flow of nitrogen for 45 min in a closed vial. Subsequently, the reaction was continued for 22 h in an oil bath at 70 °C. Afterwards, the polymers were purified by dialysis (MWCO: 3500 Da) in THF. The solvent was changed two times each day for 3 days. The obtained polymers were characterized accordingly by NMR spectroscopy (see below), size exclusion chromatography (SEC; see Table S3 and Figures S11–S16, Supporting Information), elemental analysis, DSC, and TGA (see Table S2 and Figures S17, S18, S24, and S25, Supporting Information).

#### *2.1.2. Polymer Networks*

For synthesis of polymer networks, in case of **PN1** and **PN2,** BMA and for **PN3** and **PN4** 2-EHMA, the desired amount of monomer **2**, AIBN and triethylene glycol dimethacrylate (TEGDMA) as a cross-linker were dissolved in 10 mL dry DMF in a 20 mL microwave vial. The exact amounts of all used monomers and reagents are summarized in (see Table S1, Supporting Information). The monomer-to-initiator ratio for all polymerizations was 100 to 1. The reaction mixture was purged with a flow of nitrogen for 45 min in a closed vial. Subsequently, the reaction was continued for 22 h in an oil bath at 70 °C. Afterwards, the polymers were purified by dialysis (MWCO: 3500 Da) in THF. The solvent was changed two times each day for 3 days. All polymers were characterized in detail by elemental analysis, DSC and TGA (see Table S2 and Figures S19 and S26, Supporting Information).

**P1**: $^1$H NMR (300 MHz, $CDCl_3$): $\delta$ = 0.95–1.90 (m, 392 H), 2.88–3.20 (m, 7H, —$N(CH_3)_2$), 3.94 (s, 63 H, —$OCH_2$), 7.14–7.30 (m, 2H, Ar—H), 7.71 (s, 1H, C═CH), 7.91 (d, 2H, Ar—H) ppm.

**P2**: $^1$H NMR (300 MHz, $CDCl_3$): $\delta$ = 0.88–1.94 (m, 195 H), 2.89–3.21 (m, 8H, —$N(CH_3)_2$), 3.95 (s, 31 H, —$OCH_2$), 7.11–7.32 (m, 2H, Ar—H), 7.73 (s, 1H, C═CH), 7.91 (d, 2H, Ar—H) ppm.

**P3**: $^1$H NMR (300 MHz, $CDCl_3$): $\delta$ = 0.87–1.96 (m, 105 H), 2.87–3.20 (m, 8H, —$N(CH_3)_2$), 3.94 (s, 16 H, —$OCH_2$), 7.10–7.30 (m, 2H, Ar—H), 7.72 (s, 1H, C═CH), 7.90 (d, 2H, Ar—H) ppm.

**P4**: $^1$H NMR (300 MHz, $CDCl_3$): $\delta$ = 0.89–1.89 (m, 714 H), 2.88–3.22 (m, 67H, —$N(CH_3)_2$), 3.83 (s, 70 H, —$OCH_2$), 7.10–7.31 (m, 2H, Ar—H), 7.72 (s, 1H, C═CH), 7.89 (d, 2H, Ar—H) ppm.

**P5**: $^1$H NMR (300 MHz, $CDCl_3$): $\delta$ = 0.90–1.91 (m, 334 H), 2.90–3.21 (m, 7H, —$N(CH_3)_2$), 3.84 (s, 32 H, —$OCH_2$), 7.15–7.29 (m, 2H, Ar—H), 7.72 (s, 1H, C═CH), 7.91 (d, 2H, Ar—H) ppm.

**P6**: $^1$H NMR (300 MHz, $CDCl_3$): $\delta$ = 0.90–1.97 (m, 159 H), 2.88–3.20 (m, 8H, —$N(CH_3)_2$), 3.83 (s, 15 H, —$OCH_2$), 7.12–7.31 (m, 2H, Ar—H), 7.72 (s, 1H, C═CH), 7.89 (d, 2H, Ar—H) ppm.

### 2.2. Cross-Linking via Thiol-ene Chemistry

#### *2.2.1. Cross-Linking with 1,10-Decanedithiol*

An amount of 600 mg of the corresponding polymer (Table S3, Supporting Information) was dissolved (**P1**–**P6**) or swollen (**PN1** – **PN4**) in 3 mL of dichloromethane. Subsequently, in another vial, a second solution containing the desired amount (added via previously prepared stock solution of each compound in dichloromethane) of thiol, 1.9 mol% of 1,8-diazabicyclo [5.4.0] undec-7-ene (DBU), and 1 wt% ascorbic acid-6-palmitate (AA6P) were dissolved in dichloromethane (total volume of the second solution: 1 mL) (see Table S4, Supporting Information). The resulting solution was added to the vial contain the polymer. Afterwards, the solvent was allowed to be evaporated at room temperature and the resulting cross-linked polymers **(SMP1 – SMP10)** were annealed overnight at 60 °C in the drying oven and, subsequently, characterized accordingly by elemental analysis, DSC and TGA (see Table S5 and Figures S20–S23 and S27–S30, Supporting Information).

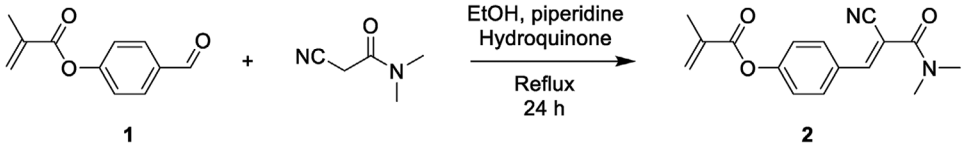


**Scheme 1.** Schematic representation of the synthesis of monomer **2** – the Michael acceptor.

**Table 1.** Overview of the dissolving experiments of polymer network **SMP4**.

| Experiment | *m* [mg] (SMP 4) | *V* [mL] (DMF) | *T* [°C] |
|---|---|---|---|
| 1 | 222 | 5 | 22 |
| 2 | 225 | 5 | 50 |
| 3 | 182 | 5 | 100 |

#### *2.2.2. Cross-Linking with 2,2′-(Ethylenedioxy)diethanethiol*

An amount of 600 mg of **PN1** or **PN3** was swollen in 3 mL of dichloromethane. Then, the desired amount of 2,2′-(ethylenedioxy) diethanethiol, 1.9 mol% of DBU, and 1 wt% AA6P were added via previously prepared stock solution of each compound in dichloromethane (see Table S4, Supporting Information). Afterwards, the solvent was allowed to be evaporated at room temperature and the resulting cross-linked polymers (**SMP11** and **SMP12**) were annealed overnight at 60 °C in the drying oven subsequently, characterized accordingly by elemental analysis, DSC and TGA (see Table S5 and Figures S23 and S30, Supporting Information). Exemplarily, the swelling behavior of **SMP7** and **SMP11** was determined in comparison with **PN1** (see Experimental Section in the Supporting Information).

### 2.3. Dissolving of Polymer Network

The polymer network **SMP4** was placed in microwave vial and DMF was added. Afterwards, the vial was capped and the mixture was heated to a certain temperature for 1 h. Before and after the reaction, a photo of each reaction mixture was taken (see Figure S55, Supporting Information). All amounts are listed in **Table 1**.

## 3. Results and Discussion

### 3.1. Synthesis of Monomer and Polymers

The reversible thiol-ene reaction of benzylcyanoacetamides and thiols was used as the reversible cross-linker within the polymer networks. Therefore, the Michael acceptor monomer was synthesized by a Knoevenagel reaction using 4-formylphenyl methacrylate (1) and 2-cyano-*N,N*-dimethylacetamide according to a literature reported protocol (**Scheme 1**).[34] The product was characterized with $^{1}$H and $^{13}$C NMR spectroscopy as well as elemental analysis (for the detailed results see Supporting Information).

For the synthesis of the polymers containing the Michael acceptor two approaches using a free radical polymerization (FRP) have been applied. Firstly, linear polymers (**P1** to **P6**) have been prepared by the copolymerization of BMA or 2-EHMA with monomer **2** in DMF and AIBN as initiator (**Scheme 2**). Both alkyl methacrylates have been selected as comonomers due to their usage in comparable studies on SMPs.[36] For both comonomers, three different polymers featuring different amount of the Michael acceptor (5%, 10%, 20%) have been prepared.

Furthermore, polymer networks (**PN1** to **PN4**) have been prepared, which feature an additional nonreversible cross-linker, TEGDMA. Hereby, two different compositions have been synthesized for each comonomer with 5% and 10%, respectively, of TEGDMA and monomer **2**. Later on, this small library of different copolymers allows the investigation of the influence of the polymer structure on the properties and the shape-memory ability.

### 3.2. Cross-Linking via Thiol-ene Reaction

The reversible binding motif was introduced by the thiol-Michael addition reaction of the *bis*benzylcyanoacetamide moieties (from monomer **2**) and different dithiols (**Scheme 3**). The linear polymers **P1–P6** were dissolved in dichloromethane and the desired amount of 1,10-decanedithiol was added. 1,8-Diazabicyclo[5.4.0]undec-7-ene (DBU) was used as a catalyst and ascorbic acid-6-palmitate (AA6P) as reducing agent in order to prevent the oxidative formation of disulfides. The formation of a gel within few minutes indicated the successful cross-linking.

For the polymer networks, the above mentioned procedure was adapted. The polymers were swollen in the solvent and an additional dithiol (2,2′-(ethylenedioxy) diethanethiol) was used for the cross-linking besides the 1,10-decanedithiol (see Table S4, Supporting Information). Hereby, swelling experiments were conducted in order to proof the successful cross-linking in the second step. For this purpose, **PN1** was compared with the cross-linked polymer networks **SMP7** and **SMP11** (for details see Supporting Information) and it could be shown that the swelling degree is reduced significantly after the second cross-linking reaction with the dithiol.

### 3.3. Raman Spectroscopic Investigation

Raman spectroscopy is a well-established method for the investigation of functional polymers in general[37] and shape-memory polymers in particular,[38,39] and we previously used this technique in multiple studies to investigate the binding conditions in the switching moiety.[17,18,36,40] Therefore, all polymer samples were studied by Raman spectroscopy to confirm the successful cross-linking via the thiol-ene reaction. Additionally, the temperature-induced reversibility of the reversible covalent bond could be studied in detail via this technique (see Scheme S1, Supporting Information, right side). For this, a Fourier-transform

 

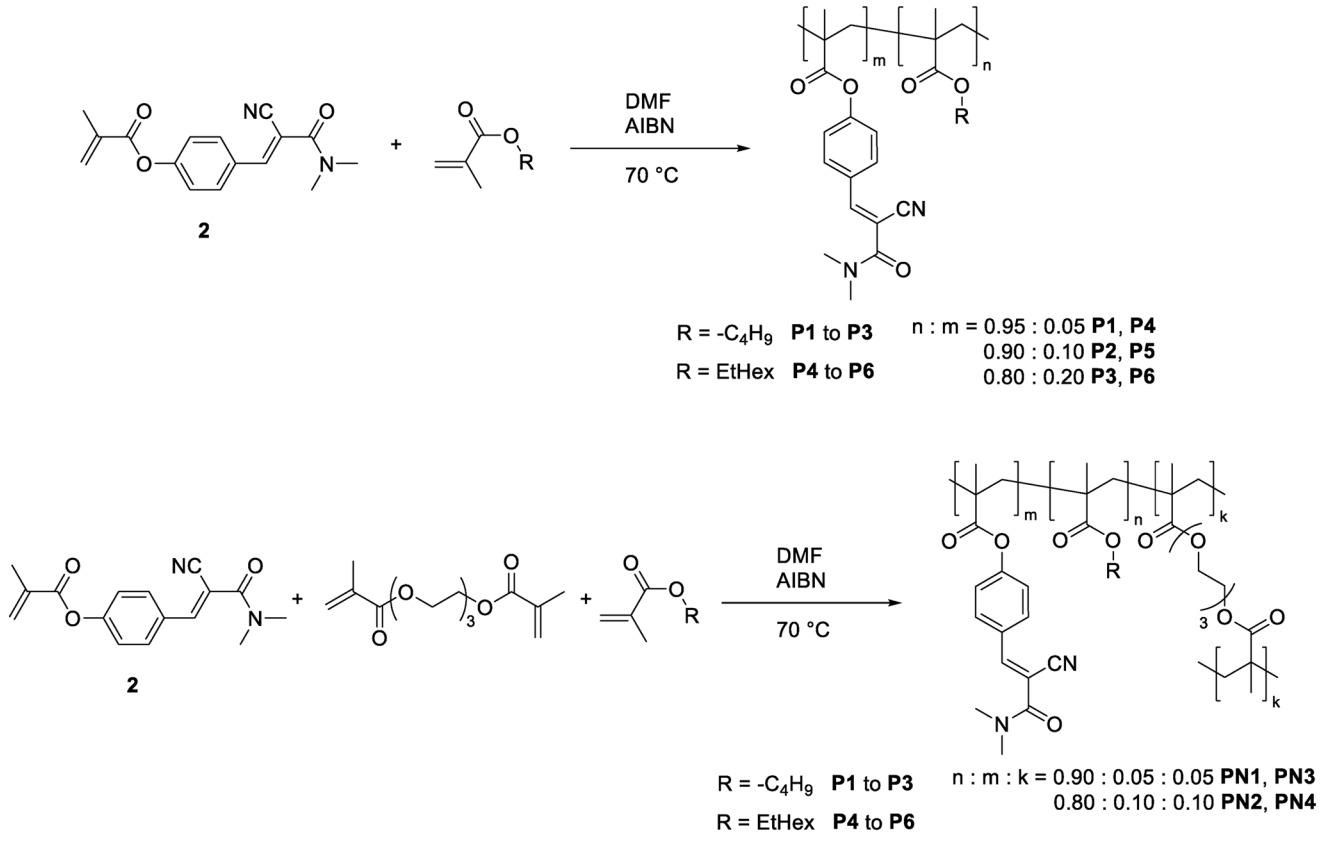


**Scheme 2.** Schematic representation of the synthesis of the linear copolymers **P1** to **P6** and of the polymer networks **PN1** to **PN4**.

(FT) based Raman spectrometer with an excitation wavelength of 1064 nm was used that offers very good wavelength stability and is insensitive to fluorescence due to excitation relatively far in the near infrared region.

**Figure 1** exemplarily shows the Raman spectra of three pairs of samples before and after the thiol-ene reaction (**PN4**/**SMP10**, **P1**/**SMP1**, and **P3**/**SMP3**) in the wavenumber region between 1500 and 2300 $cm^{-1}$, which corresponds to the region where C═C (around 1600 $cm^{-1}$) and C≡N stretching vibrations (around 2200 $cm^{-1}$) cause signals in the Raman spectrum.[41] The pair **PN4**/**SMP10** (black lines, bottom) demonstrates the expected changes for a complete reaction to the Raman spectrum: The doublet at 1580/1600 $cm^{-1}$ in the uncross-linked sample **PN4** changes to a single signal at 1603 $cm^{-1}$ and strongly decreases in intensity for the reacted sample **SMP10**. This is consistent with the vanishing of the C═C double bond that is conjugated to a benzyl moiety due to the Michael addition, which removes the second energy level causing the doublet and shortens the length of the conjugated $\pi$-electron system, which causes the strong loss in intensity. Furthermore, a shift of the signal at 2210 $cm^{-1}$ to higher wavenumbers by ≈30 $cm^{-1}$ can be observed.[41] This shift is also caused by the loss of the C═C double bond that is conjugated to the nitrile group in **PN4**. This conjugation lowers the vibrational energy of the stretching vibration, thus causing a shift of the signal to higher wavenumbers when it is removed.[41] Moreover, a loss in intensity, caused again by the shortening of the conjugated $\pi$-electron system, can be seen for this signal as well. Since the C≡N stretching vibration lies in the so-called silent region of the Raman spectrum, a region between ≈1850 and 2700 $cm^{-1}$ where only a few chemical moieties cause signals, this signal is especially interesting for further investigation as there are no overlapping signals present. The other traces in Figure 1 exemplarily show the changes to the Raman spectrum in case of only partial completion of the click reaction (**P1**/**SMP1**: red, middle; **P3**/**SMP3**: blue, top) Here, signals for both species can still be seen to varying degrees depending on the ratio of unreacted to reacted species.

With the Raman spectra recorded, it is furthermore possible to quantify the progression of the cross-linking reaction by comparing the ratios of the bands of the reacted and unreacted species. To do this, Voigt profiles were fitted to the relevant peak areas and the areas of the signals for the reacted and unreacted species were compared (detailed description of the calculation see Supporting Information). From this, the amount of reacted species for each reaction pair could be determined from the C≡N and C═C stretching region, which are tabulated in **Table 2**. All samples except for **P3**/**SMP3** have a ratio of reacted species of over 80% calculated from the C≡N and 70% from the C═C region. Samples **SMP5**, **SMP7**, and **SMP10** show full completion of the reaction indicated by vanishing intensity of the C≡N vibration for the unreacted species. In general, the values calculated from C═C and C≡N regions are in good agreement, but in some cases the value for the C═C region is significantly lower than that of the C≡N region. Since the C═C region features overlapping bands of

 

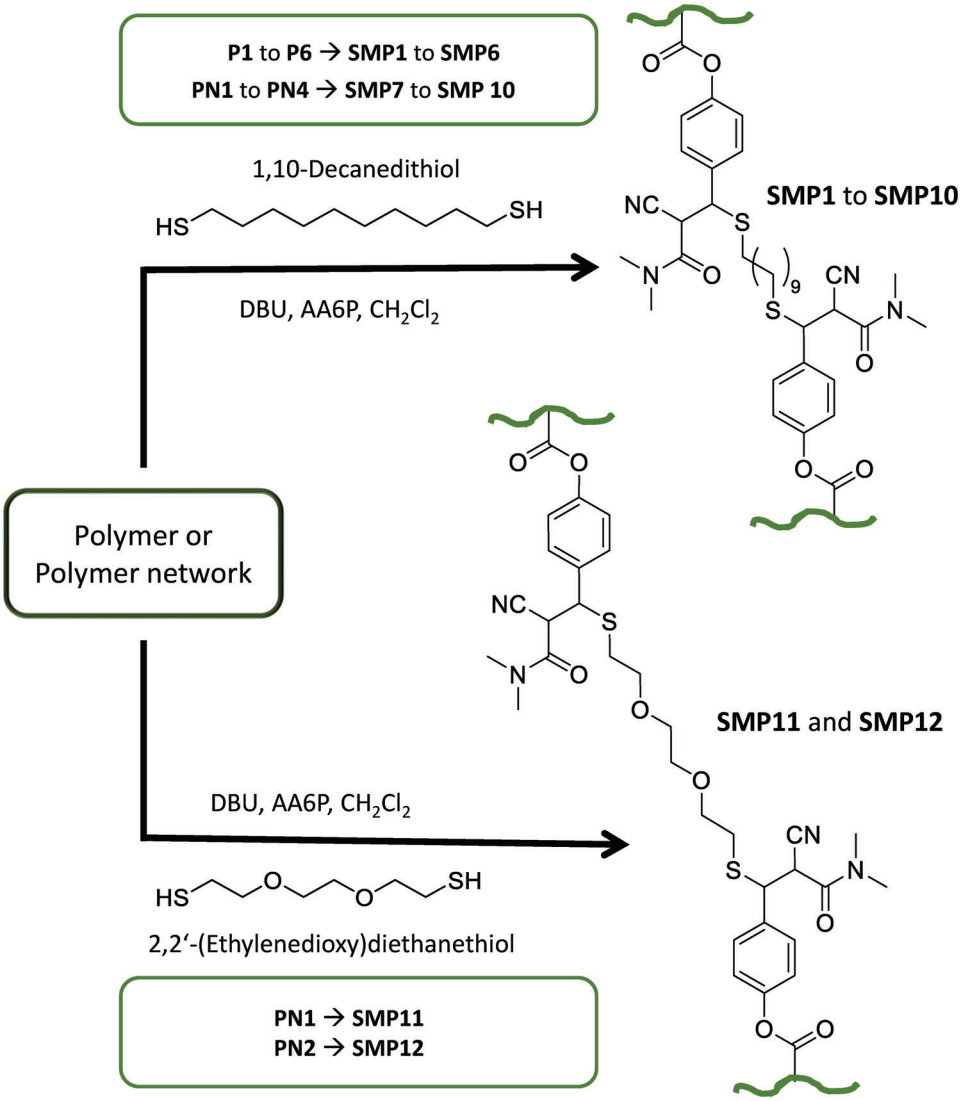


**Scheme 3.** Schematic representation of the synthesis of the polymer networks **SMP1**–**SMP12**.

the aromatic moiety and the C=C stretching vibration, while the C≡N region is free from such overlap, the values calculated from the latter should offer a better measure.

To confirm the activation of the thiol-ene functionality under elevated temperatures and, thus, support the proposed shape-memory mechanism on a molecular level, temperature-dependent Raman spectroscopy was performed exemplarily on sample **SMP9** (see Figure 1, right). It is immediately evident that the changes to the C≡N stretching region discussed previously are partially reversed under elevated temperatures above 80 °C indicating opening of the thiol-ene bond. Through the same band-fitting method it is furthermore possible to calculate the ratio of the two species for each temperature, showing a steady decrease of the amount of reacted species to ≈75% between 80 °C and 110 °C, after which it remains relatively stable up to maximum heating temperature of 125 °C, which could be a hint for a dynamic exchange of the thiol-ene moieties at these temperatures that ensures that a certain amount of reacted species is always present. Such behavior has previously been seen for a range of stimuli-responsive polymers.[42,43] The found behavior during the temperature-depending Raman spectroscopy can be connected to the results of the dynamic mechanical thermal analysis (DMTA). The value of the storage modulus continuously decreases with higher temperatures fitting to the increasing amount of open reversible bonds (Figures S38–S43, Supporting Information). Furthermore, the storage modulus and the loss modulus cross each other indicating a more flexible polymer. At higher temperatures, the storage modulus is higher compared to the loss modulus (expect **SMP2**), indicating the presence of a polymer network structure even at higher temperatures. In the case of **SMP2**, the Raman investigation revealed the lowest conversion of C=C-double bonds for the polymers studied by DMTA. The rather low content of cross-linking moieties and the further opening of the thiol-ene group at higher temperatures results in a more opened network observable by a higher loss modulus.

 

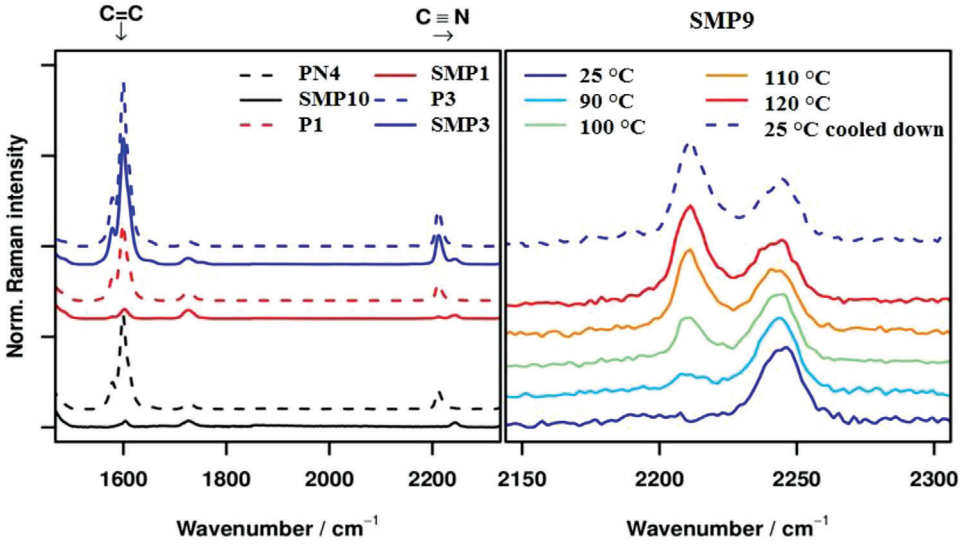


**Figure 1.** Left: Raman spectra ($\lambda_{Exc}$ = 785 nm) of three sample pairs before (dashed line) and after (solid line) the thiol-ene reaction showing varying degrees of reaction turnover. Top to bottom: **PN4**/**SMP10**, **P1**/**SMP1**, **P3**/**SMP3**. Right: Set of Raman spectra of **SMP9** during heating from room temperature to 125 °C and after cooling back down to room temperature showing the activation of the thiol-ene moiety under elevated temperatures.

**Table 2.** Calculated turnovers for the thiol-ene click reaction obtained from fitting the C≡N and C=C stretching signals in the Raman spectra of the respective sample pairs.

| Sample | Sample after thiol-ene reaction | Turnover (C≡N)% | Turnover (C=C)% |
|---|---|---|---|
| P1 | SMP1 | 90 ± 4 | 94 ± 3 |
| P2 | SMP2 | 83 ± 4 | 71 ± 3 |
| P3 | SMP3 | 50 ± 2 | 25 ± 1 |
| P4 | SMP4 | 89 ± 4 | 79 ± 3 |
| P5 | SMP5 | 101 ± 5 | 95 ± 3 |
| P6 | SMP6 | 98 ± 5 | 80 ± 3 |
| PN1 | SMP7 | 102 ± 5 | 101 ± 4 |
| PN3 | SMP9 | 93 ± 4 | 103 ± 4 |
| PN4 | SMP10 | 104 ± 5 | 101 ± 4 |

Interestingly, the ratio of reacted species did not again reach the previous level of almost 100 % upon cooling down the sample but rather remained at 75%, which can be caused by the very long and high (up to 125 °C) thermal treatment and, thus, potential side reaction of the thiols or the not complete re-cross-linking as observed also in other studies.[34,35] The TGA measurements (see Section 3.5) did not reveal a significant mass loss, e.g., induced by $H_2S$ formation.

### 3.4. Thermal Behavior of the Polymers and Polymer Networks

The obtained polymers and cross-linked networks were investigated by DSC and TGA measurements (see Figures S17–S30, Supporting information). The glass transition temperature ($T_g$) of all samples, if a $T_g$ could be detected, was found to be in a range of 25 °C to 50 °C. It could be concluded that by using BMA as main monomer for polymerization, the $T_g$ of polymers tends to the higher temperatures near to 50 °C. Instead, using 2-EHMA leads to lower $T_g$ around room temperature. This behavior was expected since it correlates well with the $T_g$s of the corresponding homopolymers.[44] In the case of **SMP6** a second, very small endothermic signal at higher temperatures (onset 115 °C, maximum at 140 °C) could be detected, which presumably results from the opening of the thiol-ene adduct in the polymer. **SMP6** features the highest amount of thiol-ene cross-linkers and, therefore, this signal could be detected only in this polymer composition. TGA measurements revealed that all polymers and cross-linked networks were stable up to 210 °C. Furthermore, the cross-linking of the initial polymers by thiols leads to a higher degradation temperature ($T_d$) and comparable $T_g$ in most of the cross-linked polymers. Interestingly, the $T_g$ is not significantly influenced by the amount of the reversible cross-linkers, i.e., the thermal properties have been successfully decoupled from the reversible covalent chemistry.

Furthermore, the polymers were investigated using temperature dependent stress relaxation measurements. For this purpose, sample **SMP4** was investigated between 25 °C and 110 °C. The stress relaxation was measured in 10 K steps and the results can be seen in **Figure 2** as well as in the supporting information (Figure S44, Supporting information). It could be revealed that the stress-relaxation behavior is strongly temperature dependent and three different regimes can be observed. Below 50 °C, the stress relaxation becomes faster with increasing temperature. This behavior resembles the expected stress relaxation of vitrimers.[22] In contrast, in the medium temperature range (60–80 °C), the stress relaxation is getting slower and a residual stress is observed. Interestingly, this behavior is similar to the stress relaxation observed for partial vitrimers, i.e., polymer networks which feature reversible moieties and permanent cross-links.[45] In the higher temperature regime, the curves are comparable to an elastomer.

 

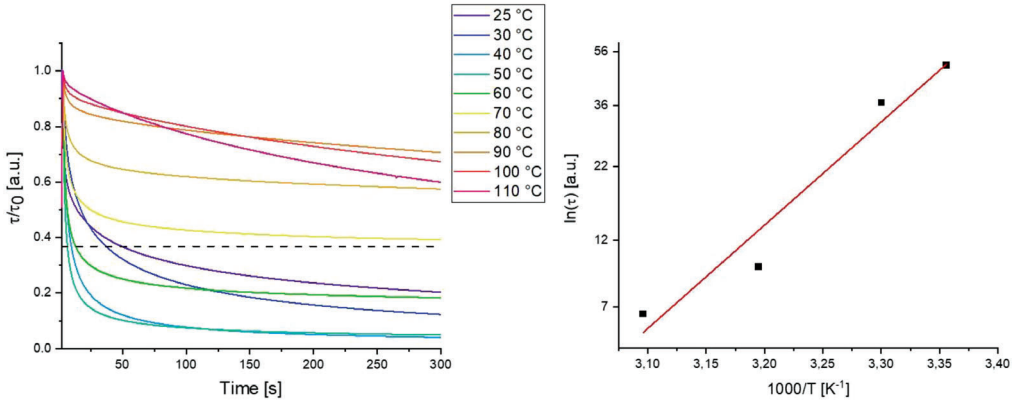


**Figure 2.** Stress relaxation measurements of **SMP4** at various temperatures (left) and the Arrhenius plot of the stress-relaxation measurements up to 50 °C (right).

First of all, we have to note that such a behavior has not been described for any reversible polymer so far. This behavior can, presumably, be explained by the two possible mechanism of the reversible bond (see Scheme S1, Supporting Information). At lower temperatures, the reversible thiol-ene bonds exchange between each other. Thus, the polymer network behaves like a vitrimer, like observed in the stress relaxation. At higher temperature, the mechanism seems to change. In literature, the change of the exchange mechanism has been described for vinylogous urethanes as reversible moiety.[46] But still the second pathway was based on the bond exchange. In our case, the second reversible reaction is the dissociation of the thiol-ene bond, which becomes more relevant at higher temperatures (as it also has been observed in the Raman measurements). Consequently, the polymer behaves first as a partial vitrimer and, finally, like an elastomer due to the reduced cross-linking density (as not all bonds are open—see also Raman results).

For the vitrimer-like behavior (up to 50 °C), we plotted the stress relaxation behavior in an Arrhenius plot and an activation energy of 70 kJ mol$^{-1}$ could be determined. This value is in the expected range compared to other vitrimers.[24]

In order to validate our hypothesis further, we performed dissolving experiments of **SMP4** in DMF (see Figure S55, Supporting information). For the associative exchange at lower temperatures, the polymer network should not be soluble in the good solvent DMF. At room temperature and even at 50 °C **SMP4** does not dissolve—like expected. At a higher temperature, 100 °C, the polymer was completely dissolved within 1 h, which is expectable considering the dissociation of the polymer network.

### 3.5. Shape-Memory Investigation

The shape-memory properties of the synthesized cross-linked networks (**SMP1** to **SMP12**) have been studied in detail. Firstly, a permanent shape (rectangular form) was prepared. For this purpose, proper amounts of synthesized cross-linked polymers were pressed at 130 °C with a pressure between 1 and 4 *t* in an adequate mold.

Subsequently, the shape-memory ability was tested by hand. For this purpose, the rectangular shape was heated up to 90 °C, twisted, and cooled down to room temperature resulting in the temporary shape. The network stayed in its new form without any changes until it was heated up again to 90 °C. Finally, the twisted shapes recovered to the permanent form at 90 °C in just a few minutes (**Figure 3**).

All synthesized cross-linked networks were investigated regarding their shape-memory ability; however, only six samples indicated appropriate recovery and fixation properties. Hereby, networks containing BMA, monomer **2** (5% or 10%) and cross-linker (TEGDMA) (5% or 10%) were broken during deformation.

In contrast, the polymer network **SMP9** containing 2-EHMA, the thiol-ene cross-linker (5%) and nonreversible cross-linker (TEGDMA) (5%) illustrated a different behavior and was able to recover the shape. However, if the content of the thiol-ene moiety and the cross-linker (TEGDMA) increased to 10%, the rectangular shape was broken again.

Interestingly, the formulations without the permanent cross-linker (TEGDMA), i.e., **SMP1**, **SMP2**, and **SMP4** lead to better performance in the shape-memory experiment. This behavior indicates that an additional stable phase (provided by a classical cross-linker) is not required due to the partial reversibility of the used thiol-ene reaction (see also Raman studies in Section 3.4). The standard design with the permanent cross-linker leads in this case even to a decreased shape-memory ability due to a higher brittleness of the material. Furthermore, an increase of the amount of thiol-ene cross-linker also reduces the ability of shape-recovery since the samples gets more and more brittle and tends to break during deformation. The use of 2,2′-(ethylenedioxy) diethanethiol as cross-linker leads to more flexible polymers and, consequently, to deformation without breaking while maintaining the shape-memory behavior. This behavior could potentially be explained by a better mixability of the different polymer segments leading to a better polymer sample.

TMA was performed in order quantify the shape-memory behavior (see Figures S31–S37 (Supporting Information); all values are listed in Table S7, Supporting Information). In this experiment, it was possible to calculate the strain fixity ($R_f$) and the strain recovery rate ($R_r$) (Equations1 and 2). $R_f$ represents the capability of a polymer to fix a mechanical deformation, while the $R_r$ is the efficiency of the reformation of the permanent shape.[47] The resulting TMA plots of cross-linked networks, at a switching

 

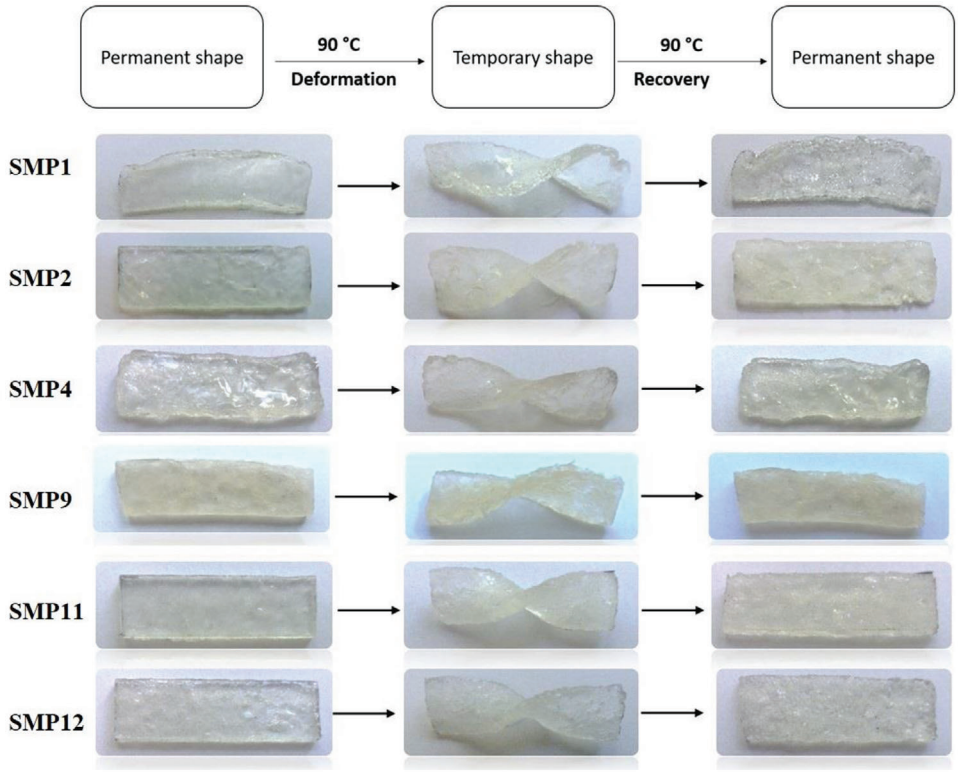


**Figure 3.** Photo series of the shape-memory test of different networks (test performed at a temperature of 90 °C).

**Table 3.** Calculated strain fixity and recovery rates for the cross-linked networks.

| Polymer | Strain fixity rate $R_f$ [%] | | | | Strain recovery rate $R_r$ [%] | | | |
|---|---|---|---|---|---|---|---|---|
| | 1st | 2nd | 3rd | 4th | 1st | 2nd | 3rd | 4th |
| SMP1 | 96.3 | 96.2 | 96.3 | 96.0 | 96.0 | 97.7 | 98.1 | 98.3 |
| SMP2 | 97.5 | 97.2 | 96.9 | 96.2 | 96.9 | 98.2 | 98.4 | 98.7 |
| SMP4 | 92.2 | 91.2 | 90.3 | 89.4 | 93.8 | 96.0 | 96.1 | 96.8 |
| SMP4[a)] | 85.3 | 85.9 | 85.9 | 85.8 | 95.3 | 95.8 | 96.0 | 96.1 |
| SMP9 | 91.6 | 92.1 | 91.9 | 91.7 | 94.3 | 99.7 | 89.8 | 93.9 |
| SMP11 | 98.1 | 98.0 | 97.5 | 97.7 | 97.9 | 98.2 | 98.4 | 99.0 |
| SMP12 | 87.0 | 86.2 | 85.7 | 85.2 | 96.0 | 97.8 | 98.3 | 98.4 |

[a)] After the recycling (shredded and hot pressed).

temperature of 90 °C, are illustrated in the supporting information.

$$R_f\ (N) = \frac{\gamma_u\,(N)}{\gamma_m\,(N)} \times 100\% \quad (1)$$

$$R_r\ (N) = \frac{\gamma_m\,(N) - \gamma_p\,(N)}{\gamma_m\,(N) - \gamma_p\,(N-1)} \times 100\% \quad (2)$$

All calculated values of the strain recovery and fixity rates are summarized in **Table 3**. The measurements indicate suitable shape-memory abilities for most of the studied polymer networks. All samples featured $R_f$-values above 90% except **SMP12**. **SMP9** and **SMP12** [2-EHMA, TEGDMA (5%), and thiol-ene cross-linker (5%)] are cross-linked with different thiols (1,10-decanedithiol for **SMP9** and 2,2′-(ethylenedioxy) diethanethiol for **SMP12**). $R_f$ for **SMP9** is higher compared to **SMP12**. The more polar cross-linker 2,2′-(ethylenedioxy)diethanethiol seems to be not as effective.

Counterintuitively, the cross-linking with 1,10-decanedithiol leads to better shape-memory abilities, if the initial polymers are synthesized without the additional cross-linker (TEGDMA) (**SMP1**, **SMP2**, and **SMP3**).

Furthermore, a direct comparison of **SMP1** and **SMP4** (same polymer design, expect main monomer: BMA for **SMP1** and EHMA for **SMP4**) indicates that the switching is presumably based on the reversible thiol-ene reaction. The onset of the recovery during the TMA measurement can be found at ≈60 °C in both cases independent from the glass transition of the polymer. Thus, the reversible bonding seems to be responsible for the shape-recovery process and its onset is already at 60 °C, which fits to literature reported studies for the thiol-ene reversibility.[34] In our case, the temperature-dependent Raman spectroscopy also shows that the onset of the bond opening is in the range of 60 °C or slightly higher (see **Figure 4**), which is well-fitting to the shape-memory results obtained by TMA.

To investigate the influence of a possible recycling/reprocessing on the shape-memory abilities an additional experiment was performed with **SMP4**. After the first TMA test, the sample was shredded and hot pressed (under the same conditions as before). Subsequently, a second TMA measurement

 

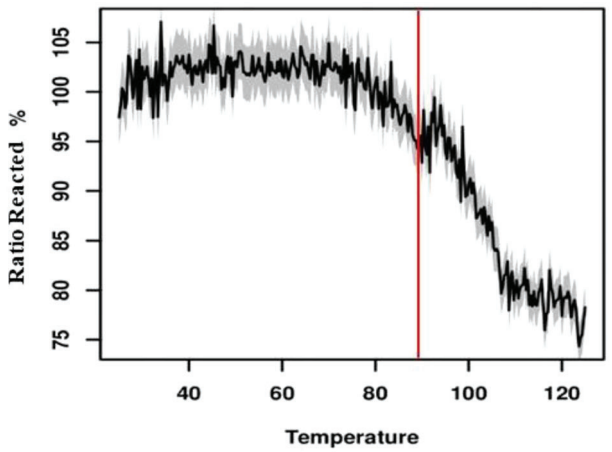


**Figure 4.** Calculated ratios of reacted species in **SMP9** during heating from room temperature to 125 °C (black line) and standard deviation (grey background) (red line is indicating the switching temperature of 90 °C).

was conducted with the recycled sample (see Figures S33 and S34, Supporting Information; values are listed in Table S7, Supporting Information).

## 4. Conclusion

We herein presented the use of reversible thiol-ene chemistry as switching moiety in shape-memory polymers. Two different polymer network types have been prepared—one being exclusively cross-linked via the reversible moiety and a second containing an additional covalent cross-linker as stable phase. All polymers have been studied in detail by DSC, TGA, and TMA measurements revealing their thermal and mechanical properties. Two different alkyl methylacrylates (butyl methacrylate or 2-ethylhexyl methacrylate) have been used as comonomers resulting in different $T_g$ for the materials. However, the use of the reversible covalent bond as switching unit lead to a switching process independent of the respective $T_g$. Some of the studied SMPs revealed excellent shape-memory ability. Noteworthy, the polymer networks without the permanent cross-linker have proven to be the best systems here. This effect is caused by the partial reversibility of the thiol-ene reaction, which was also proven by Raman spectroscopy and stress relaxation measurements. Interestingly, the measurements also revealed that the thermal behavior is presumably associated with two reversible mechanisms. At lower temperatures the polymer behaves like a vitrimer and at higher temperature the reversible bonds tend to open inducing a partial decross-linking. Our study shows that dissociative reversible covalent bonds featuring a partial reversibility are interesting systems for the design of SMPs with less materials required (no permanent cross-linker needed).

## Supporting Information

Supporting Information is available from the Wiley Online Library or from the author.

## Acknowledgements

The authors would like to thank the Carl-Zeiss foundation (Perspektiven 2019) and the Deutsche Forschungsgemeinschaft (DFG; HA 6306/7-1; project number: 398304946 and funding within the framework of FOR 5301 FuncHeal) for funding.

## Conflict of Interest

The authors declare no conflict of interest.

## Data Availability Statement

The data that support the findings of this study are available from the corresponding author upon reasonable request.

## Keywords

(reversible) Michael addition, reversible covalent polymer networks, (reversible) thiol-ene reaction, shape-memory polymers

Received: January 28, 2023
Revised: March 27, 2023
Published online: April 25, 2023

[1] R. V. Bellamkonda, *Nat. Mater.* **2008**, *7*, 347.
[2] M. Wei, Y. Gao, X. Li, M. J. Serpe, *Polym. Chem.* **2017**, *8*, 127.
[3] S. Wang, M. W. Urban, *Nat. Rev. Mater.* **2020**, *5*, 562.
[4] M. D. Hager, S. Bode, C. Weber, U. S. Schubert, *Prog. Polym. Sci.* **2015**, *49–50*, 3.
[5] A. Lendlein, O. E. C. Gould, *Nat. Rev. Mater.* **2019**, *4*, 116.
[6] W. Small, IV, P. Singhal, T. S. Wilson, D. J. Maitland, *J. Mater. Chem.* **2010**, *20*, 3356.
[7] M. Behl, A. Lendlein, *Mater. Today* **2007**, *10*, 20.
[8] J. Hu, Y. Zhu, H. Huang, J. Lu, *Prog. Polym. Sci.* **2012**, *37*, 1720.
[9] C. Wang, Y. Zhang, J. Li, Z. Yang, Q. Wang, T. Wang, S. Li, S. Chen, X. Zhang, *Eur. Polym. J.* **2020**, *123*, 109393.
[10] A. Lendlein, A. M. Schmidt, M. Schroeter, R. Langer, *J. Polym. Sci., Part A: Polym. Chem.* **2005**, *43*, 1369.
[11] B. K. Kim, S. Y. Lee, M. Xu, *Polymer* **1996**, *37*, 5781.
[12] M. Ahmad, J. Luo, B. Xu, H. Purnawali, P. J. King, P. R. Chalker, Y. Fu, W. Huang, M. Miraftab, *Macromol. Chem. Phys.* **2011**, *212*, 592.
[13] W. Miao, W. Zou, Y. Luo, N. Zheng, Q. Zhao, T. Xie, *Polym. Chem.* **2020**, *11*, 1369.
[14] M. M. Perera, N. Ayres, *Polym. Chem.* **2020**, *11*, 1410.
[15] Z. Li, R. Yu, B. Guo, *ACS Appl. Bio Mater.* **2021**, *4*, 5926.
[16] Z.-C. Jiang, Y.-Y. Xiao, Y. Kang, M. Pan, B.-J. Li, S. Zhang, *ACS Appl. Mater. Interfaces* **2017**, *9*, 20276.
[17] J. Meurer, J. Hniopek, T. Bätz, S. Zechel, M. Enke, J. Vitz, M. Schmitt, J. Popp, M. D. Hager, U. S. Schubert, *Adv. Mater.* **2021**, *33*, 2006655.
[18] J. Meurer, R. H. Kampes, T. Bätz, J. Hniopek, O. Müschke, J. Kimmig, S. Zechel, M. Schmitt, J. Popp, M. D. Hager, U. S. Schubert, *Adv. Funct. Mater.* **2022**, *32*, 2207313.
[19] J. M. Winne, L. Leibler, F. E. Du Prez, *Polym. Chem.* **2019**, *10*, 6091.
[20] C. J. Kloxin, C. N. Bowman, *Chem. Soc. Rev.* **2013**, *42*, 7161.
[21] B. R. Elling, W. R. Dichtel, *ACS Cent. Sci.* **2020**, *6*, 1488.
[22] W. Denissen, J. M. Winne, F. E. Du Prez, *Chem. Sci.* **2016**, *7*, 30.
[23] D. Montarnal, M. Capelot, F. Tournilhac, L. Leibler, *Science* **2011**, *334*, 965.
[24] W. Denissen, G. Rivero, R. Nicolaÿ, L. Leibler, J. M. Winne, F. E. Du Prez, *Adv. Funct. Mater.* **2015**, *25*, 2451.

 

[25] B. Briou, B. Améduri, B. Boutevin, *Chem. Soc. Rev.* **2021**, *50*, 11055.
[26] M. K. Mcbride, B. T. Worrell, T. Brown, L. M. Cox, N. Sowan, C. Wang, M. Podgorski, A. M. Martinez, C. N. Bowman, *Annu. Rev. Chem. Biomol. Eng.* **2019**, *10*, 175.
[27] F. Gamardella, F. Guerrero, S. De La Flor, X. Ramis, A. Serra, *Eur. Polym. J.* **2020**, *122*, 109361.
[28] Z. Fang, N. Zheng, Q. Zhao, T. Xie, *ACS Appl. Mater. Interfaces* **2017**, *9*, 22077.
[29] P. Chakma, D. Konkolewicz, *Angew. Chem., Int. Ed.* **2019**, *58*, 9682.
[30] Q. Zhao, H. J. Qi, T. Xie, *Prog. Polym. Sci.* **2015**, *49-50*, 79.
[31] K. Inoue, M. Yamashiro, M. Iji, *J. Appl. Polym. Sci.* **2009**, *112*, 876.
[32] B. Zhao, H. Mei, G. Hang, L. Li, S. Zheng, *Polymer* **2021**, *230*, 124042.
[33] X. Kuang, G. Liu, X. Dong, D. Wang, *Polymer* **2016**, *84*, 1.
[34] N. Kuhl, R. Geitner, J. Vitz, S. Bode, M. Schmitt, J. Popp, U. S. Schubert, M. D. Hager, *J. Appl. Polym. Sci.* **2017**, *134*.
[35] N. Kuhl, R. Geitner, R. K. Bose, S. Bode, B. Dietzek, M. Schmitt, J. Popp, S. J. Garcia, S. Van Der Zwaag, U. S. Schubert, M. D. Hager, *Macromol. Chem. Phys.* **2016**, *217*, 2541.
[36] J. Meurer, T. Bätz, J. Hniopek, S. Zechel, M. Schmitt, J. Popp, M. D. Hager, U. S. Schubert, *J. Mater. Chem. A* **2021**, *9*, 15051.
[37] S. Bode, M. Enke, M. Hernandez, R. K. Bose, A. M. Grande, S. van der Zwaag, U. S. Schubert, S. J. Garcia, M. D. Hager, *Adv. Polym. Sci.* **2016**, *273*, 113.
[38] S. Maity, C. Ramanan, F. Ariese, R. C. I. Mackenzie, E. Von Hauff, *Adv. Electron. Mater.* **2022**, *8*, 2101208.
[39] L. V. Elliott, E. E. Salzman, J. R. Greer, *Adv. Funct. Mater.* **2021**, *31*, 2008380.
[40] J. Meurer, T. Bätz, J. Hniopek, C. Bernt, S. Zechel, M. Schmitt, J. Popp, M. D. Hager, U. S. Schubert, *J. Mater. Chem. A* **2022**, *10*, 25106.
[41] G. Socrates, *Infrared and Raman Characteristic Group Frequencies: Tables and Charts*, 3rd ed., Wiley, Chichester **2004**.
[42] J. Meurer, J. Hniopek, S. Zechel, M. Enke, J. Vitz, M. Schmitt, J. Popp, M. D. Hager, U. S. Schubert, *Polymers* **2019**, *11*, 1889.
[43] S. Zechel, R. Geitner, M. Abend, M. Siegmann, M. Enke, N. Kuhl, M. Klein, J. Vitz, S. Gräfe, B. Dietzek, M. Schmitt, J. Popp, U. S. Schubert, M. D. Hager, *NPG Asia Mater.* **2017**, *9*, e420.
[44] F. Fleischhaker, A. P. Haehnel, A. M. Misske, M. Blanchot, S. Haremza, C. Barner-Kowollik, *Macromol. Chem. Phys.* **2014**, *215*, 1192.
[45] F. Meng, M. O. Saed, E. M. Terentjev, *Macromolecules* **2019**, *52*, 7423.
[46] M. Guerre, C. Taplan, R. Nicolaÿ, J. M. Winne, F. E. Du Prez, *J. Am. Chem. Soc.* **2018**, *140*, 13272.
[47] J. Meurer, J. A. Rodriguez Agudo, S. Zechel, M. D. Hager, U. S. Schubert, *Macromol. Chem. Phys.* **2021**, *222*, 2000462.

 